



Article

Comparison of Two Light Wavelengths ($\lambda = 660$ nm and $\lambda = 780$ nm) in the Repair Process of Oral Mucositis Induced by Ionizing Radiation: Clinical and Microscopic Evaluations in Rats

Maíra Franco Andrade ¹, Ariane Venzon Naia Sardo ¹, Carolina Benetti ^{1,2}, Leticia Bonfante Sicchieri ^{1,3}, Luciana Corrêa ⁴  and Denise Maria Zzell ^{1,*} 

¹ Center for Lasers and Applications, Nuclear and Energy Research Institute, São Paulo CEP 05508-000, Brazil

² Center of Engineering, Modeling and Applied Social Sciences, Federal University of ABC, São Bernardo do Campo CEP 09606-045, Brazil

³ Preparatory School for Army Cadets, Campinas CEP 13070-091, Brazil

⁴ School of Dentistry, University of São Paulo, São Paulo CEP 05508-000, Brazil

* Correspondence: zzell@usp.br

Abstract: Photobiomodulation (PBM) has been clinically used for the prevention and treatment of oral mucositis (OM). The effect of red and near-infrared wavelengths on OM repair is still misunderstood. The aim of this study was to compare the clinical effect and tissue changes caused by 660 nm and 780 nm exposure in an experimental model of OM. Rats were submitted to gamma irradiation for induction of OM lesions and treated with 660 nm or 780 nm lasers with the same dosimetry parameters (30 mW, 7.5 J/cm², 10 s, spot size = 0.04 mm, irradiation every two days). Clinical assessment of OM severity and histopathological analyses was performed after 8, 14, and 20 days of the ionizing radiation. OM severity was reduced in the PBM groups, especially when the red laser was used. The histopathological pattern was similar between the PBM groups, showing advanced re-epithelization and more pronounced angiogenesis and collagen deposition compared to the control. The 660 nm group showed a greater collagen matrix area than the 780 nm group at 14 days. In conclusion, PBM at 660 nm and 780 nm improved the repair of ionizing radiation-induced OM. Both wavelengths activated the angiogenesis and collagen deposition, but these tissue effects were more pronounced when 660 nm was used.

Keywords: laser photobiomodulation; radiotherapy; oral mucositis



Citation: Andrade, M.F.; Sardo, A.V.N.; Benetti, C.; Sicchieri, L.B.; Corrêa, L.; Zzell, D.M. Comparison of Two Light Wavelengths ($\lambda = 660$ nm and $\lambda = 780$ nm) in the Repair Process of Oral Mucositis Induced by Ionizing Radiation: Clinical and Microscopic Evaluations in Rats. *Photonics* **2023**, *10*, 16. <https://doi.org/10.3390/photonics10010016>

Received: 11 October 2022

Revised: 7 December 2022

Accepted: 9 December 2022

Published: 24 December 2022



Copyright: © 2022 by the authors. Licensee MDPI, Basel, Switzerland. This article is an open access article distributed under the terms and conditions of the Creative Commons Attribution (CC BY) license (<https://creativecommons.org/licenses/by/4.0/>).

1. Introduction

Oral mucositis (OM) is one of the main complications of nonsurgical treatments against head and neck cancer, and is derived from chemotherapy, ionizing radiation, or a combination of these two therapeutic modalities [1]. Radiotherapy-induced OM is a consequence of direct damage to the DNA strands present in the cells of the oral epithelium, evolving to the generation of oxygen free radicals, activation of nuclear factors, such as NF-kB, and consequent tissue degradation processes [2–4].

OM shows different clinical stages, ranging from mild erythema to severe ulcerations. The epithelial discontinuity leaves the patient more vulnerable to opportunistic infections and to severe pain, which may limit the function of the oral cavity. The risk for systemic dissemination of these infections and the nutrition disturbances caused by OM may increase hospital costs [5,6].

Although there is not yet a universal protocol for the clinical management of this condition, the current available therapies involve mainly local and systemic anti-inflammatory and analgesic drugs, oral hygiene protocols, and photobiomodulation (PBM) [7]. PBM

shows efficacy in the clinical management of OM, either in cases caused by chemotherapy [8,9] or radiotherapy [10,11], or in cases where OM was caused by the use of combination of these two treatment modalities [12]. PBM is currently considered the standard treatment for OM lesions, especially because it does not cause the systemic toxicity that pharmacological treatment can generate [1,13,14].

In general, the clinical protocols for oral mucosa repair preconize the intraoral use of red lasers (630 nm or 660 nm) under an energy density up to 6 J/cm² [11,14]. PBM with near-infrared lasers (780 nm, 815–830 nm) has also demonstrated good outcomes for OM prevention [15], combined or not with red lasers [16,17], although the number of clinical studies is lower than those focused on red lasers. In addition, the literature is heterogeneous with regard to PBM parameters, such as beam diameter, energy and power densities, and irradiation mode (scan or spot) [1,13,14].

In this study, we decided to compare the clinical effect and tissue changes caused by 660 nm and 780 nm exposure in an experimental model of OM induced by ionizing radiation. For this, the same laser protocols were used to infer the direct role of each wavelength on the different phases of oral mucosa repair. The premise was to understand the differences between the two wavelengths in terms of clinical outcomes and microscopic changes in oral mucosa to contribute to the establishment of more accurate PBM protocols.

2. Materials and Methods

The study was previously approved by the IPEN Animal Facility, IPEN Ethics Committee-CNEN/SP (94/11/CEUA-IPEN/SP). The research was carried out at the Biophotonics Laboratory from the IPEN/USP Lasers and Applications Center.

2.1. Oral Mucositis Model and Experimental Groups

Fifty-four male Wistar rats, with approximately 350 g body mass, were used for the experimental groups. The animals were kept in cages (up to 30 animals in each) and maintained under 12 h light/dark cycles. Water and pelleted commercial feed (Nuvilab[®], Nuvital, Brazil) were offered ad libitum.

Prior to the start of the rat experiment, a dosimetry of a Cobalt-60 (⁶⁰Co) panoramic source localized in the Radiation Technology Center (CTR-IPEN/SP) was performed to obtain the dose rate and to establish the lead shielding conformation. An online FSH-260 silicon photodiode dosimeter, associated with an electronic outside the radiation chamber, was positioned at the source. The air dose rate was used for dosimeter calibration, and then the distance from the source and the lead thickness required for radiation shielding were tested.

The ionizing radiation dosimetry required to induce OM in rats was obtained from previously published studies [18,19] with minor adaptations. A lead thickness of 10 cm was the best shielding for the body of animals, positioned 20 cm from the source. At this distance, a dose rate of 0.60 Gy/min was obtained, with an initial exposure time of 33 min and total dose of 20 Gy delivered to the tissue. Three blocks of lead, 5 cm thick, were used to protect the trunk and lower limbs of the animal, aiming to expose only the head region to the radiation. During radiation exposure, the animals were anesthetized with intraperitoneal injection of ketamine (75 mg/kg) and xylazine (10 mg/kg). They were then distributed radially to the ionizing radiation source with a focal length of 20 cm.

After ionizing radiation, the animals were randomly divided into three groups: for the control, animals without PBM (n = 16); for the 660 nm group, animals exposed to a PBM with $\lambda = 660$ nm (n = 21); and for the 780 nm group, animals exposed to a PBM with $\lambda = 780$ nm (n = 21). The animals were further divided into three periods for clinical evaluation and tissue collection: 8, 14 and 20 days (four animals in each experimental time for the control group, and seven animals in each experimental time for the PBM groups). Two animals died, one from the control and one from the 660 nm group, totaling to 52 animals at the end of the experiment (Table 1). The study design is illustrated in Figure 1.

Table 1. Laser parameters and number of animals in each experimental period.

Groups and Laser Parameters	Number of Animals			
	Day 8	Day14	Day 20	Total
$\lambda = 780 \text{ nm}$, 30 mW, 7.5 J/cm ² , 10 s, spot size = 0.04 mm \varnothing ; Irradiation = every 48 h	07	07	07	21
$\Lambda = 660 \text{ nm}$, 30 mW, 7.5 J/cm ² , 10 s, spot size = 0.04 mm \varnothing ; Irradiation = 48/48 h	07	07	06	20
Control	04	04	03	11
Total	18	18	16	52

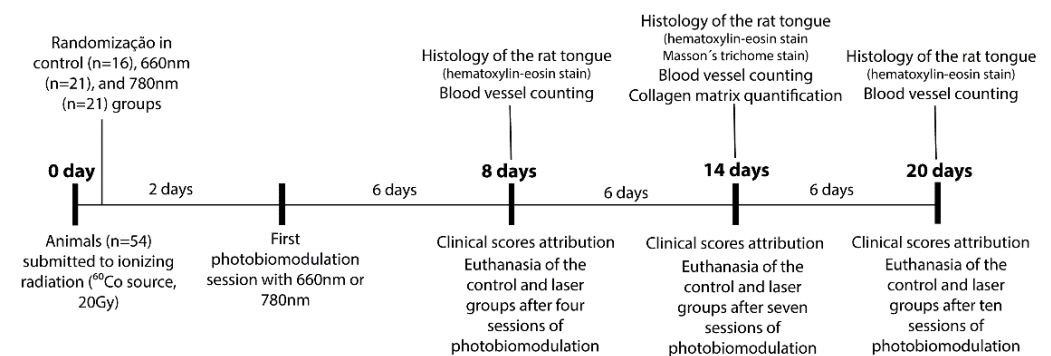


Figure 1. Study methodology in accordance with the experimental periods.

2.2. Photobiomodulation

The animals were anesthetized according to the protocol previously described. Then, they were placed in a horizontal support for the PBM procedure. A GaAlAs diode laser irradiation (MMOptics®, Brazil) was performed in the tongue mucosa every two days. Five irradiation points were chosen to cover the entire exposed surface of the tongue, three in the base and two in the tongue apex. The laser parameters are listed in Table 1. The control group was subjected to the same manipulation and procedures performed for the PBM groups, including intraperitoneal anesthesia, maintenance in the horizontal support, and PBM simulation with the laser probe positioned on the tongue surface, but without illumination.

2.3. Clinical Assessment

OM severity was assessed by a clinical examination of the tongue, in which edema and erythema, extension of the ulcerated surface, and extension of the pseudomembrane formation were graded using the scores described in Table 2.

Each animal was evaluated clinically at the time of laser irradiation. After anesthesia, the animal operator photographed the rat tongue using the same illumination, 2 focus magnification, and the same focus distance from the tongue surface. Each animal was photographed three times; the best image was chosen for further analysis by two independent examiners, who were blinded to the groups and experimental times. Prior to the definitive registering of the clinical scores, these examiners were calibrated by observing and applying the grades to random images of the rat tongue in which different clinical situations were presented. The groups and experimental periods were concealed. This process was repeated three times, and the third evaluation was submitted to the agreement kappa test. A 100% agreement between the examiners was achieved. The definitive examiners' grades were then analyzed in terms of the relative frequency of each score.

Table 2. Clinical scores for assessment of oral mucositis severity.

Grades	Description
<i>Edema and erythema</i>	
0	Absence of tumor and redness in the tongue
1	Absence of tumor; slight redness in some areas of the tongue
2	Presence of tumor; slight redness in some areas of the tongue
3	Presence of tumor; intense redness in some areas of the tongue
4	Presence of tumor; intense redness in the entire tongue surface
<i>Pseudomembrane formation</i>	
0	Absence of pseudomembrane
1	Isolated pseudomembrane
2	Continuous pseudomembrane covering $\leq 20\%$ of the tongue surface
3	Continuous pseudomembrane covering 21% to 50% of the tongue surface
4	Continuous pseudomembrane covering $\geq 51\%$ of the tongue surface
<i>Ulcerated surface</i>	
0	Absence of ulcers
1	One small ulcer (unifocal)
2	Multiple small ulcers with a total extension of $\leq 20\%$ of tongue surface
3	Multiple small ulcers with a total extension of $\geq 21\%$ of the tongue surface
4	Coalescent ulcers with a total extension of $\leq 30\%$ of the tongue surface
5	Coalescent ulcers with a total extension of 31% to 50% of the tongue surface
6	Coalescent ulcers with a total extension of $\geq 51\%$ of the tongue surface

2.4. Euthanasia and Histopathological Analysis

Euthanasia was performed at 8, 14 and 20 days with an overdose of the anesthetics applied intraperitoneally, with subsequent finalization in a CO₂ chamber. The rat tongue was extirpated using a surgical scalpel blade, washed in physiological solution, and fixed in 4% paraformaldehyde solution for 24 h. Laboratorial processing for paraffin-embedding was performed for all the samples. Histological sections (3 μ m thick) were obtained and stained with hematoxylin and eosin (HE). Specimens at the experimental time of 14 days were also stained with Masson's trichrome, for the analysis of collagen deposition, which was more evident at this moment of the repair process than at 8 and 20 days.

An experienced pathologist examined the histological sections, analyzing the following tissue elements: necrosis, inflammatory infiltrate, re-epithelization, collagen deposition, angiogenesis, cellularity, and extracellular remodeling.

A semi-automated quantification of the collagen matrix and manual blood vessel counting were performed for each group and experimental period. For this, histological fields were digitized using a Leica DM2500 microscope (Leica Biosystems, Wetzlar, Germany) with a Leica DFC 295 camera (Leica Biosystems, Wetzlar, Germany) and a LAS[®] acquisition and morphometry program (Leica Biosystems, Wetzlar, Germany). The same light intensity was used for all scans. The scanned images were kept in RGB format, with a resolution of 2048 \times 1536 pixels and a jpg extension.

For collagen matrix quantification, three fields in the ventral surface and three fields in the dorsal surface of the tongue stained with Masson's trichrome were digitized ($\times 100$ original magnification) by an operator who did not know the groups and experimental periods. The images were then submitted to a color deconvolution method using Image J software, which segmented the image into red and blue colors, equivalent to the muscle and collagen fibers, respectively. The area occupied by the blue color (collagen fibers) was quantified by means of blue tone selection; this area was then normalized by the total area of the field, obtaining a mean percentage of the collagen area presented in the histological section.

For blood vessel counting, 10 HE-stained fields ($\times 400$ original magnification) localized in the lamina propria of the ventral and dorsal tongue surfaces were digitized by an operator who did not know the groups and experimental periods. Blood vessels with visible lumens

and various diameters were manually counted using Image J software. The total vessel number was then obtained by summing the vessels counted in each field.

2.5. Statistical Tests

The data normality of the clinical scores was assessed using Shapiro–Wilk’s test. As the data did not show normality, the groups were compared using the nonparametric Kruskal–Wallis test, followed by Dunn’s test. The blood vessel counts did not achieve a parametric distribution and were analyzed by the same statistical tests. The percentage of collagen matrices exhibited a parametric distribution, and the groups were compared using ANOVA followed by Tukey’s test. For the statistical analyses, GraphPad Prism 5[®] was used. The level of significance was set at 5%.

3. Results

3.1. Clinical Outcomes

Figure 2 shows the clinical aspect of the rat tongue in each group and experimental period. At 8 days, in the control group, the tongue exhibited intense erythema and edema, as well as a confluent ulceration. In the 660 nm and 780 nm groups, the erythema was more discrete compared to the control, and pseudomembrane formation and a restricted ulcerated surface were noted. At 14 days, in all the groups, the erythema was mitigated and the ulcerated area was reduced, mainly in the laser groups. At 20 days, in all the groups, the tongue was completely healed.

3.1.1. Edema and Erythema

Figure 3A shows the grade frequency for edema and erythema. On day 8, all animals in the control group had the highest edema and/or erythema scores. In the 660 nm group, 100% of the animals exhibited a score of 3, while in the group treated with the 780 nm laser, this score was attributed to 70% of the animals. In both groups the differences were statistically significant in relation to the control ($p < 0.05$). At 14 days, the laser groups already had some animals with a score of 0 (35% in the 660 nm group and 25% in the 780 nm group), in contrast to the control group, where these signs persisted to severe degrees in all animals. The difference was statistically significant when the control was compared to the 660 nm group. On the 20th day, in the laser groups, some animals were absent of erythema and edema or evolved to score 1. The differences in relation to the control were not statistically significant during this period.

3.1.2. Pseudomembrane Formation

Figure 3B shows the grade frequency for pseudomembrane formation. At 8 days, the 660 nm group showed the highest scores (score 4–56.2%, score 3–47.4%), showing significant differences in relation to the control ($p < 0.05$) but not in relation to the 780 nm group. On day 14, in the control group, 87% of the animals showed low pseudomembrane scores, whereas in the laser groups most of the animals did not exhibit this clinical sign. This difference was statistically significant for both laser groups ($p < 0.05$). At 20 days, none of the animals showed pseudomembrane.

3.1.3. Ulcerated Surface

Figure 3C shows the grade frequency for the ulcerated surface. On day 8, an ulceration score of 6 was observed in 54.4% of the animals in the control group, compared to 10.5% and 30.0% of the animals in the 660 nm and 780 nm laser groups, respectively. On day 14, in all the groups the ulceration score dropped to 4, with some animals in the laser group without this clinical sign. In the 660 nm group, 25.5% of the animals showed complete re-epithelization, whereas in the 780 nm group only 7.1% of the animals healed the oral mucosa. At 20 days, 80% of the animals in the 660 nm group exhibited complete re-epithelization, compared to 57.3% in the 780 nm laser group, and 25% in the control group. In none of the experimental periods were the differences statistically significant.

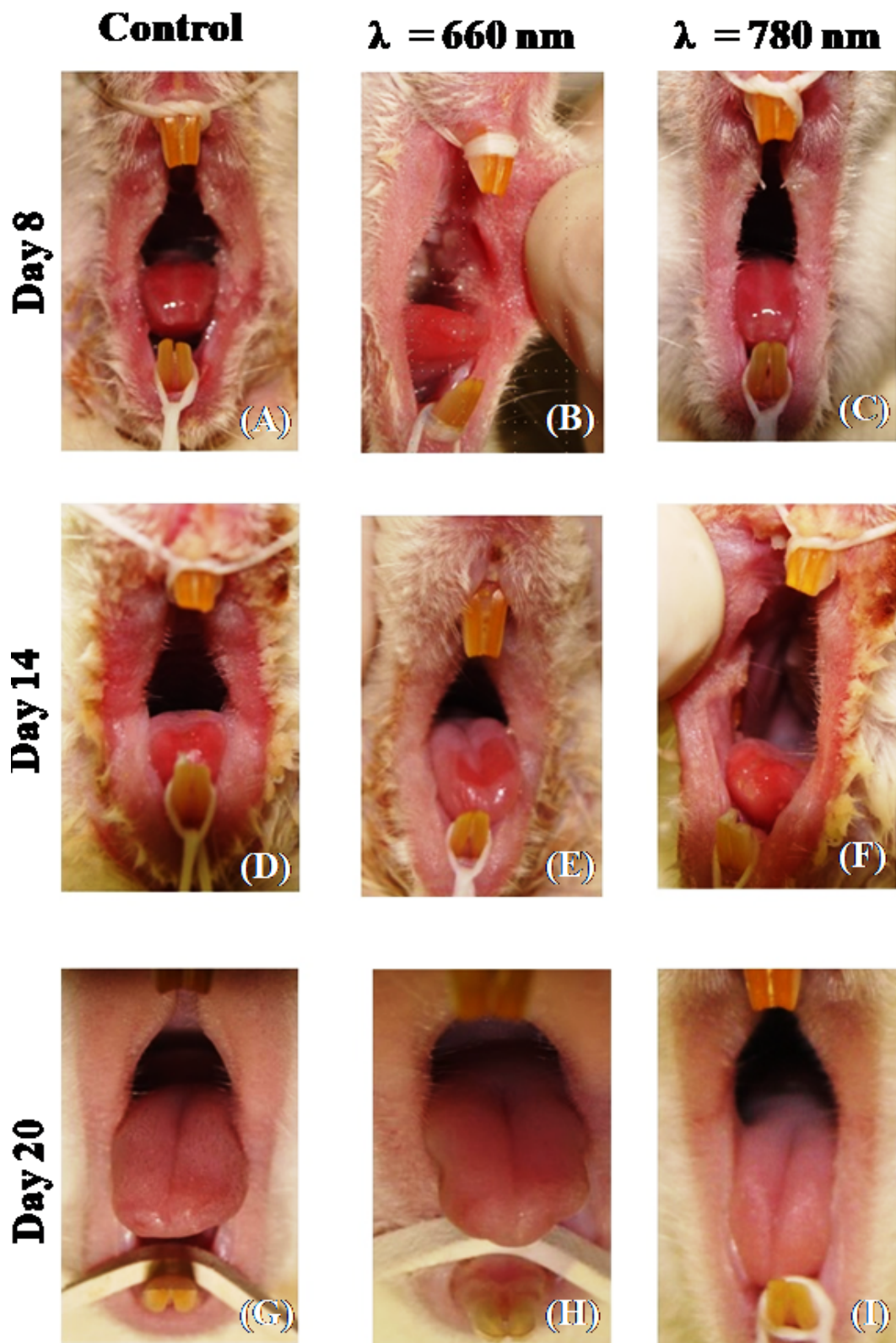


Figure 2. Representative images of the clinical aspect of the tongue after induction of oral mucositis with ionizing radiation (control group, (A,D,G)). The tongue received photobiomodulation with $\lambda = 660 \text{ nm}$ (660 nm group, B, E and H) or $\lambda = 780 \text{ nm}$ (780 nm group, (C,F,I)). The tongue was analyzed after 8 days (A–C), 14 days (D–F), and 20 days (G–I) of ionizing radiation.

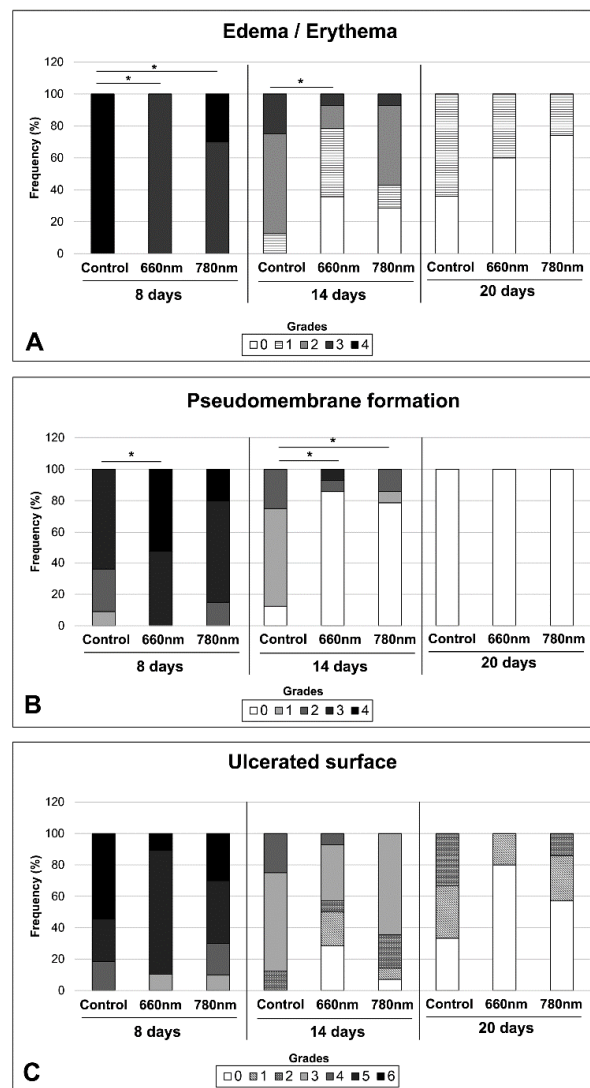


Figure 3. Frequency of severity grades for edema/erythema (A), pseudomembrane formation (B) and ulcerated surface (C) attributed to oral mucositis induced with ionizing radiation (control group) and treated with photobiomodulation performed with $\lambda = 660$ nm (660 nm group) and $\lambda = 780$ nm (780 nm group). The tongue was analyzed after 8, 14, and 20 days of ionizing radiation. The grade description for each clinical variable is shown in Table 1. * $p < 0.05$ (Kruskal–Wallis test, followed by Tukey’s test).

3.2. Histopathological Evaluation

Figure 4 shows the histopathological aspect of the tongue mucosa in each group and experimental period. In the control group, intense epithelial atrophy on both the dorsal and ventral surfaces was observed at 8 days (Figure 4A), with a focal area of ulceration at the transition from the ventral to dorsal surface. At the base of the ulcer, the granulation tissue was composed of hyperemic blood vessels, fibroblasts, and fibrillar extracellular matrices. The ulcerated surface exhibited a large area of necrosis, with the presence of polymorphonuclear cell infiltrate. In the 660 nm group at the same period (Figure 4B), the histopathological aspect was similar to the control, but the vessels were more dilated, and the collagen deposition was more exuberant, especially near the ulcer surface. The 780 nm group (Figure 4C) also showed the same characteristics as the two other groups, with the difference that the vasodilatation was less pronounced, especially when compared to the 660 nm group.

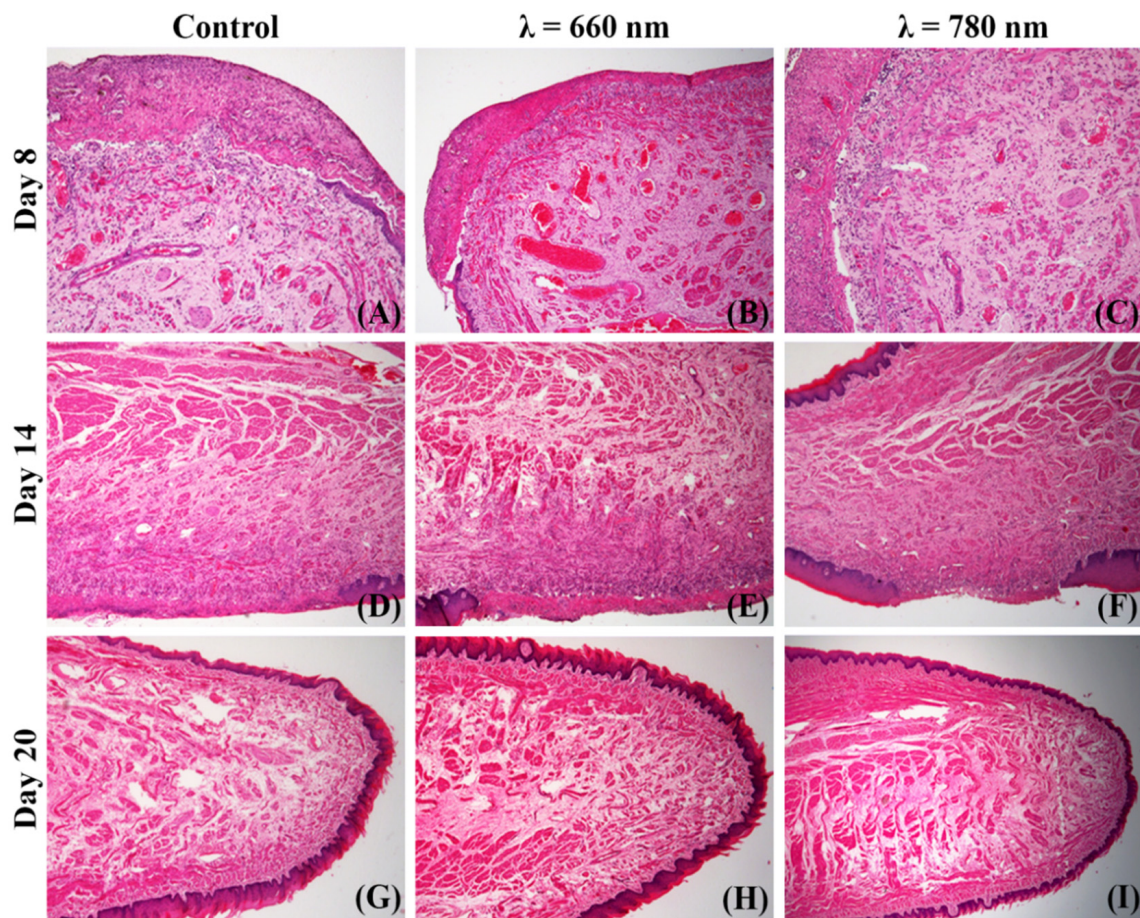


Figure 4. Representative histological fields showing the repair process of ionizing radiation-induced oral mucositis (control group, (A,D,G)) treated with $\lambda = 660$ nm photobiomodulation (660 nm group, (B,E,H)) or $\lambda = 780$ nm photobiomodulation (780 nm group, (C,F,I)). The repair process was registered after 8 (A–C), 14 (D–F) and 20 days (G–I) of ionizing radiation (hematoxylin-eosin, $\times 20$ or $\times 50$ original magnification).

At 14 days, the control group (Figure 4D) showed an advanced repair process, with resorption of superficial necrosis, partial reconstruction of the connective tissue by mature granulation tissue, and intense re-epithelization. In the submucosa, the muscle fibers were regenerating, and no sign of fibrosis was noted. In the 660 nm group at the same period (Figure 4E), re-epithelization and muscle regeneration were similar to those observed in the control group, but the granulation tissue exhibited a more abundant collagen matrix and more pronounced angiogenesis. The 780 nm group (Figure 4F) had the same histopathological pattern, with a predominance of re-epithelization, collagen deposition, and angiogenesis.

At 20 days, in the control group (Figure 4G) the tongue mucosa was completely healed, with no sign of fibrosis. The 660 nm (Figure 4H) and 780 nm (Figure 4I) groups also exhibited complete repair of the oral mucosa, but more collagen deposition was noted in the comparison to the control, mainly between the muscle fibers generating a thick endomysium.

3.3. Blood Vessel Counting

Figure 5 shows the values for blood vessel density in accordance with the groups and time periods. At 8 days, the control showed a significantly lower vessel density than the 660 nm ($p < 0.05$) and 780 nm ($p < 0.05$) groups. After 14 days, although the control showed the lowest values compared to the laser groups, the differences were not significant. At

20 days, the 660 nm and 780 nm groups showed a higher vessel density than the control, but the differences were statistically significant only for the 660 nm group ($p < 0.05$).

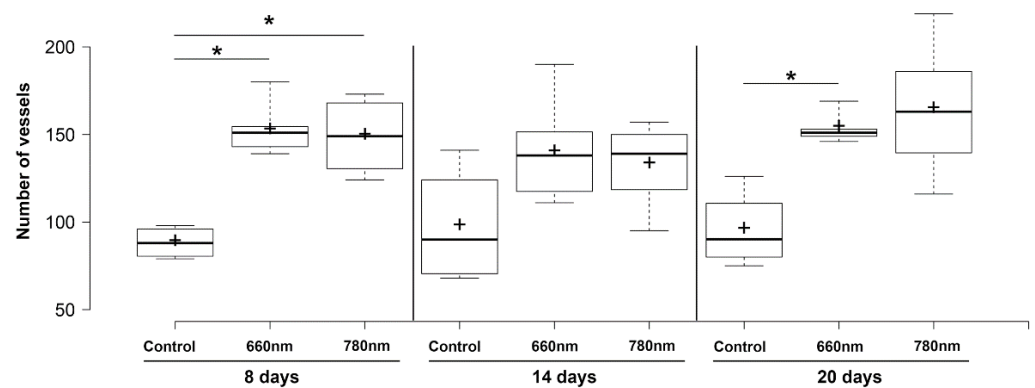


Figure 5. Boxplot for blood vessel counting in each group and experimental time. Center line in the boxes —median; +—mean; box limits—25th and 75th percentiles; whiskers—minimum and maximum values. * $p < 0.05$ (Kruskal–Wallis’ test followed by Dunn’s test).

3.4. Collagen Matrix Measurement

Figure 6 shows the collagen matrix presented in each group at 14 days. The mean percentage of the collagen fibers area is shown in Table 3. Analyzing the quantification of the collagen matrix in the lamina propria, the 660 nm group showed the highest concentration of collagen fibers, showing significant differences in relation to the 780 nm ($p < 0.01$) and control ($p < 0.01$). The collagen area at the 780 nm was also higher than that of the control ($p < 0.01$). In the submucosa, there were no significant differences in collagen area between the groups, but for the muscle area, the laser groups showed higher values than the control ($p < 0.05$ for both laser groups).

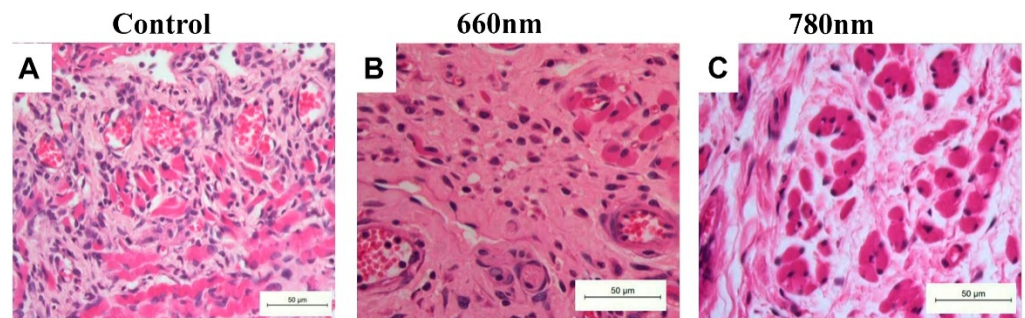


Figure 6. Representative histological sections of the collagen matrix in each group at 14 days (hematoxylin-eosin, $\times 400$ original magnification). (A) Control group showing collagen fibers disposable in various directions and with high cellularity, suggesting poor remodeling. (B) The 660 nm group exhibiting a dense collagen matrix, without fiber patterns and fewer cellularity. (C) The 780 nm group showing a dense but more remodeled collagen matrix between the muscle fibers.

Table 3. Mean percentage \pm standard deviation of collagen fibers and muscle tissue in samples of oral mucositis after 14 days of ionizing radiation.

Group	Mucosa	Submucosa	
	Collagen (%)	Collagen (%)	Muscle (%)
Control Group	16.93 \pm 5 A	16.93 \pm 5	47.89 \pm 11 B
Laser 660 nm	35.69 \pm 8 B	17.46 \pm 8	52.95 \pm 6 A
Laser 780 nm	28.13 \pm 5 C	15.3 \pm 9	53.62 \pm 7 A

Different letters indicate statistically significant differences (ANOVA test followed by Tukey’s test).

4. Discussion

In this study, we demonstrated, for the first time, that PBM with the same energy density and wavelengths of 660 nm or 780 nm exerted similar effects during the repair process of OM induced by ionizing radiation. The two wavelengths showed clinical efficacy for reducing inflammatory signs and ulceration. However, some discrete differences between the two wavelengths were noted in the histopathology analysis, especially regarding the more pronounced effect of the red laser on the blood vessel density and collagen deposition in some phases of tissue repair.

The clinical outcomes found in the OM model adopted in the current study were compatible with those described in previous studies [18,19]. The OM was clinically recognized in the animal through erythema and edema presented at 3 days after ionizing irradiation. The onset of epithelial erosion was observed from the sixth day after irradiation. The dorsal apex of the tongue was the first ulcerated region, probably due to the direct contact of the tongue apex with the incisors, generating direct and constant friction in the attempt to seize the food. The highest severity of OM occurred between days 8 and 12, in which coalescent ulcers were noted on the tongue surface.

At 8 days, the animals exposed to 660 nm and 780 nm had high degrees of erythema and edema, and microscopically, vasodilatation was notorious. It is most likely that the great absorption of 660 nm and 780 nm by chromophores localized in the blood improved vasodilatation and vascular permeability at 8 days. In addition, during this experimental period, the blood vessel density was greater in the laser group than in the controls, suggesting that the vasodilatation induced by PBM facilitated vessel visualization, and consequently influenced the blood vessel count. However, after 14 days, both 660 nm and 780 nm wavelengths were considered efficacious in mitigating erythema and edema; at this period, most animals of the control group exhibited these inflammatory signs and the animals with PBM did not. At 660 nm, this effect was more pronounced, considering the severity scores adopted in the current study. The success of PBM in negatively modulating the inflammatory process of the mucosa has also been described by recent studies [20,21], mainly by decreasing the expression of pro-inflammatory factors in oral mucositis [4,22,23].

Both laser groups showed a significant reduction in pseudomembrane formation, which occurred clearly at 14 days. This finding suggests that PBM reduced the necrotic ulcer surface and improved re-epithelization. Microscopically, the two wavelengths promoted efficient and comparable necrotic tissue absorption, supporting the clinical findings. Macrophages with the M1 phenotype are mainly responsible for necrotic tissue phagocytosis. There is some evidence that the effect of 660 nm on macrophages with this phenotype is different from that induced by near-infrared wavelengths; 660 nm induces more pro-inflammatory release by macrophages than 780 nm [24] and more nitric oxide than 808 nm [25]. Although we observed a similar efficiency in the reduction of tissue necrosis by the two wavelengths, it is important to consider different mechanisms of action determined by the red and near-infrared wavelengths in terms of macrophage activation and pseudomembrane absorption.

A marked effect of PBM is the reduction in the ulcerated surface, mitigating oral pain and reducing the risk for secondary infection [5,26,27]. In the current study, both PBM groups were efficacious in reducing the ulcerated surface area, mainly after 14 and 20 days, although the differences in relation to the control were not significant, probably because the number of animals was insufficient. Microscopically, both groups showed exuberant re-epithelization at these experimental periods and mature granulation tissue, which is important for keratinocyte migration. Considering that the red wavelength can activate keratinocyte differentiation [28] and seems to be more sensitive to keratinocyte proliferation than near-infrared wavelengths [29], further *in vivo* studies are necessary to elucidate the differences between the red and near-infrared wavelengths in the process of OM re-epithelization.

The 660 nm group showed the highest vascular density not only at 8 days, as discussed above, but also at 20 days. The increase in vascularity at this later repair stage is suggestive

of angiogenesis. The 780 nm group also showed high mean values of vascular density, but the differences were not significant in relation to the control due to the data variance. The use of PBM has been previously associated in the literature with an increase in vascular components during healing processes [30,31]. A study showed that a red laser (650 nm) was more efficient in angiogenesis induction than a near-infrared laser (808 nm), leading to the cycle progression of the endothelial cell, calcium influx, nitric oxide production, and an increase in levels of the vascular endothelial growth factor associated with the macrophage M2 phenotype [32]. In another experiment with skin flaps in rats, 660 nm induced angiogenesis via activation of hypoxia inducible factor α , whereas 780 nm caused a direct increase in the vascular endothelial growth factor [31]. Therefore, both wavelengths can activate angiogenesis through different pathways, with 660 nm having more pronounced effect considering the conditions of OM repair and previous exposure to ionizing radiation.

The red laser also promoted higher collagen production than 780 nm, although this near-infrared wavelength also induced more collagenization than the control. The 660 nm wavelength, as already discussed in other studies published in the literature, has a great influence on stimulating the ability of fibroblasts to produce collagen [33,34]. An investigation compared the use of 630 nm and 850 nm LEDs on cutaneous repair and concluded that red LEDs induced more collagenization and intense expression of tumor growth factor β than near-infrared LEDs, but both wavelengths were efficacious in improving skin healing [35]. This trend can be extrapolated to OM repair, mainly considering the connective tissue near the epithelium.

An important aspect of the current study was that both wavelengths were applied with the same laser parameters, with 7.5 J/cm² per point. The energy densities used for OM vary in the literature, being conditioned, among other factors, on the OM severity, laser or LED equipment characteristics, and specific protocols established locally. An energy density up to 6 J/cm² was considered safe for oncologic patients [11,14], but recent protocols adopted higher energy densities for OM (11.1 J/cm²) and have also been considered safe [36]. In the current study we adopted an intermediate energy density commonly applied for the induction of OM repair, to improve the extrapolation of the results to the patient's clinical situation.

5. Conclusions

PBM performed with 7.5 J/cm² and wavelengths of 660 nm and 780 nm improved the repair of ionizing radiation-induced OM by reducing the inflammatory signs and stimulating the absorption of the necrotic tissue surface, mainly when 660 nm was applied. Both wavelengths activated angiogenesis and collagen deposition, but these tissue effects were more pronounced when 660 nm was used.

Author Contributions: Conceptualization, D.M.Z., M.F.A. and L.C.; methodology, M.F.A., C.B., L.B.S.; formal analysis, L.B.S. and D.M.Z.; writing—original draft preparation, A.V.N.S.; writing—review and editing, D.M.Z. and L.C.; supervision, D.M.Z.; project administration, D.M.Z.; funding acquisition, D.M.Z. and L.C. All authors have read and agreed to the published version of the manuscript.

Funding: Fundação de Amparo à Pesquisa do Estado de São Paulo (FAPESP) (17/50332-0; 13/26113-6; 17/07519-2), Coordenação de Aperfeiçoamento de Pessoal de Nível Superior/Programa de Cooperação Acadêmica em Defesa Nacional (CAPES/PROCAD) 88881.068505/2014-01 and Conselho Nacional de Desenvolvimento Científico e Tecnológico (CNPq) (INTC-465763/2014-6, PQ- 314517/2021-9).

Institutional Review Board Statement: The animal study protocol was approved by the Institutional Ethics Committee of Instituto de Pesquisas Energéticas e Nucleares protocol code 94/11/CEUA-IPEN/SP.

Data Availability Statement: The data that support the findings of this study are available from the corresponding author, [D.M.Z.], upon reasonable request.

Acknowledgments: This work was supported by Fundação de Amparo à Pesquisa do Estado de São Paulo (FAPESP) (17/50332-0; 13/26113-6; 17/07519-2), Coordenação de Aperfeiçoamento de Pessoal de Nível Superior/ Programa de Cooperação Acadêmica em Defesa Nacional (CAPES/PROCAD)

88881.068505/2014-01 and Conselho Nacional de Desenvolvimento Científico e Tecnológico (CNPq) (INTC-465763/2014-6, PQ- 314517/2021-9).

Conflicts of Interest: The authors declare no conflict of interest.

References

1. Elad, S.; Cheng, K.K.F.; Lalla, R.V.; Yarom, N.; Hong, C.; Logan, R.M.; Bowen, J.; Gibson, R.; Saunders, D.P.; Zadik, Y.; et al. MASCC/ISOO Clinical Practice Guidelines for the Management of Mucositis Secondary to Cancer Therapy. *Cancer* **2020**, *126*, 4423–4431. [[CrossRef](#)] [[PubMed](#)]
2. Sonis, S.T. The Pathobiology of Mucositis. *Nat. Rev. Cancer* **2004**, *4*, 277–284. [[CrossRef](#)]
3. Epstein, J.B.; Thariat, J.; Bensadoun, R.-J.; Barasch, A.; Murphy, B.A.; Kolnick, L.; Popplewell, L.; Maghami, E. Oral Complications of Cancer and Cancer Therapy. *CA Cancer J. Clin.* **2012**, *62*, 400–422. [[CrossRef](#)] [[PubMed](#)]
4. Curra, M.; Pellicoli, A.C.A.; Filho, N.A.K.; Ochs, G.; Matte, Ú.; Filho, M.S.; Martins, M.A.T.; Martins, M.D. Photobiomodulation Reduces Oral Mucositis by Modulating NF-KB. *J. Biomed. Opt.* **2015**, *20*, 125008. [[CrossRef](#)] [[PubMed](#)]
5. Antunes, H.S.; Schluckebier, L.F.; Herchenhorn, D.; Small, I.A.; Araújo, C.M.M.; Viégas, C.M.P.; Rampini, M.P.; Ferreira, E.M.S.; Dias, F.L.; Teich, V.; et al. Cost-Effectiveness of Low-Level Laser Therapy (LLLT) in Head and Neck Cancer Patients Receiving Concurrent Chemoradiation. *Oral Oncol.* **2016**, *52*, 85–90. [[CrossRef](#)] [[PubMed](#)]
6. Sonis, S.T. Oral Mucositis. *Anticancer Drugs* **2011**, *22*, 607–612. [[CrossRef](#)] [[PubMed](#)]
7. Hong, C.H.L.; Gueiros, L.A.; Fulton, J.S.; Cheng, K.K.F.; Kandwal, A.; Galiti, D.; Fall-Dickson, J.M.; Johansen, J.; Ameringer, S.; Kataoka, T.; et al. Systematic Review of Basic Oral Care for the Management of Oral Mucositis in Cancer Patients and Clinical Practice Guidelines. *Support. Care Cancer* **2019**, *27*, 3949–3967. [[CrossRef](#)]
8. Chaveli-López, B.; Bagán-Sebastián, J.V. Treatment of Oral Mucositis Due to Chemotherapy. *J. Clin. Exp. Dent.* **2016**, *8*, e201–e209. [[CrossRef](#)]
9. Leite Cavalcanti, A.; José de Macêdo, D.; Suely Barros Dantas, F.; dos Santos Menezes, K.; Filipe Bezerra Silva, D.; Alves de Melo Junior, W.; Fabia Cabral Cavalcanti, A. Evaluation of Oral Mucositis Occurrence in Oncologic Patients under Antineoplastic Therapy Submitted to the Low-Level Laser Coadjuvant Therapy. *J. Clin. Med.* **2018**, *7*, 90. [[CrossRef](#)]
10. Gautam, A.P.; Fernandes, D.J.; Vidyasagar, M.S.; Maiya, A.G.; Guddattu, V. Low Level Laser Therapy against Radiation Induced Oral Mucositis in Elderly Head and Neck Cancer Patients—a Randomized Placebo Controlled Trial. *J. Photochem. Photobiol. B Biol.* **2015**, *144*, 51–56. [[CrossRef](#)]
11. Kuhn-Dall’Magro, A.; Zamboni, E.; Fontana, T.; Dogenski, L.C.; De Carli, J.P.; Dall’Magro, E.; Fornari, F. Low-Level Laser Therapy in the Management of Oral Mucositis Induced by Radiotherapy: A Randomized Double-Blind Clinical Trial. *J. Contemp. Dent. Pract.* **2022**, *23*, 31–36. [[PubMed](#)]
12. Peng, H.; Chen, B.B.; Chen, L.; Chen, Y.P.; Liu, X.; Tang, L.L.; Mao, Y.P.; Li, W.F.; Zhang, Y.; Lin, A.H.; et al. A Network Meta-Analysis in Comparing Prophylactic Treatments of Radiotherapy-Induced Oral Mucositis for Patients with Head and Neck Cancers Receiving Radiotherapy. *Oral Oncol.* **2017**, *75*, 89–94. [[CrossRef](#)] [[PubMed](#)]
13. Lalla, R.V.; Brennan, M.T.; Gordon, S.M.; Sonis, S.T.; Rosenthal, D.I.; Keefe, D.M. Oral Mucositis Due to High-Dose Chemotherapy and/or Head and Neck Radiation Therapy. *J. Natl. Cancer Inst. Monogr.* **2019**, *2019*, 17–24. [[CrossRef](#)]
14. Zadik, Y.; Arany, P.R.; Fregnani, E.R.; Bossi, P.; Antunes, H.S.; Bensadoun, R.-J.; Gueiros, L.A.; Majorana, A.; Nair, R.G.; Ranna, V.; et al. Systematic Review of Photobiomodulation for the Management of Oral Mucositis in Cancer Patients and Clinical Practice Guidelines. *Support. Care Cancer* **2019**, *27*, 3969–3983. [[CrossRef](#)] [[PubMed](#)]
15. Bensadoun, R.-J. Photobiomodulation or Low-Level Laser Therapy in the Management of Cancer Therapy-Induced Mucositis, Dermatitis and Lymphedema. *Curr. Opin. Oncol.* **2018**, *30*, 226–232. [[CrossRef](#)]
16. Soares, R.G.; Farias, L.C.; da Silva Menezes, A.S.; de Oliveira e Silva, C.S.; Tabosa, A.T.L.; Chagas, P.V.F.; Santiago, L.; Santos, S.H.S.; de Paula, A.M.B.; Guimarães, A.L.S. Treatment of Mucositis with Combined 660- and 808-Nm-Wavelength Low-Level Laser Therapy Reduced Mucositis Grade, Pain, and Use of Analgesics: A Parallel, Single-Blind, Two-Arm Controlled Study. *Lasers Med. Sci.* **2018**, *33*, 1813–1819. [[CrossRef](#)]
17. Pires Marques, E.C.; Piccolo Lopes, F.; Nascimento, I.C.; Morelli, J.; Pereira, M.V.; Machado Meiken, V.M.; Pinheiro, S.L. Photobiomodulation and Photodynamic Therapy for the Treatment of Oral Mucositis in Patients with Cancer. *Photodiagnosis Photodyn. Ther.* **2020**, *29*, 101621. [[CrossRef](#)]
18. Usumez, A.; Cengiz, B.; Oztuzcu, S.; Demir, T.; Aras, M.H.; Gutknecht, N. Effects of Laser Irradiation at Different Wavelengths (660, 810, 980, and 1,064 Nm) on Mucositis in an Animal Model of Wound Healing. *Lasers Med. Sci.* **2014**, *29*, 1807–1813. [[CrossRef](#)]
19. De Freitas Cuba, L.; Braga Filho, A.; Cherubini, K.; Salum, F.G.; Figueiredo, M.A.Z. de Topical Application of Aloe Vera and Vitamin E on Induced Ulcers on the Tongue of Rats Subjected to Radiation: Clinical and Histological Evaluation. *Support. Care Cancer* **2016**, *24*, 2557–2564. [[CrossRef](#)]
20. Musstaf, R.A.; Jenkins, D.F.L.; Jha, A.N. Assessing the Impact of Low Level Laser Therapy (LLLT) on Biological Systems: A Review. *Int. J. Radiat. Biol.* **2019**, *95*, 120–143. [[CrossRef](#)]
21. Park, I.-S.; Kim, D.-K.; Kim, J.H.; Bae, J.-S.; Kim, E.H.; Yoo, S.H.; Chung, Y.-J.; Lyu, L.; Mo, J.-H. Increased Anti-Allergic Effects of Secretome of Low-Level Light Treated Tonsil-Derived Mesenchymal Stem Cells in Allergic Rhinitis Mouse Model. *Am. J. Rhinol. Allergy* **2022**, *36*, 261–268. [[CrossRef](#)] [[PubMed](#)]

22. Oton-Leite, A.F.; Silva, G.B.L.; Morais, M.O.; Silva, T.A.; Leles, C.R.; Valadares, M.C.; Pinezi, J.C.D.; Batista, A.C.; Mendonça, E.F. Effect of Low-Level Laser Therapy on Chemoradiotherapy-Induced Oral Mucositis and Salivary Inflammatory Mediators in Head and Neck Cancer Patients. *Lasers Surg. Med.* **2015**, *47*, 296–305. [[CrossRef](#)] [[PubMed](#)]
23. Villa, A.; Sonis, S.T. Mucositis. *Curr. Opin. Oncol.* **2015**, *27*, 159–164. [[CrossRef](#)] [[PubMed](#)]
24. Fernandes, K.P.; Souza, N.H.; Mesquita-Ferrari, R.A.; Silva, D.F.; Rocha, L.A.; Alves, A.N.; de Brito Sousa, K.; Bussadori, S.K.; Hamblin, M.R.; Nunes, F.D. Photobiomodulation with 660-nm and 780-nm laser on activated J774 macrophage-like cells: Effect on M1 inflammatory markers. *J. Photochem. Photobiol. B* **2015**, *153*, 344–351. [[CrossRef](#)] [[PubMed](#)]
25. Silva, I.H.; de Andrade, S.C.; de Faria, A.B.; Fonsêca, D.D.; Gueiros, L.A.; Carvalho, A.A.; da Silva, W.T.; de Castro, R.M.; Leão, J.C. Increase in the nitric oxide release without changes in cell viability of macrophages after laser therapy with 660 and 808 nm lasers. *Lasers Med. Sci.* **2016**, *31*, 1855–1862. [[CrossRef](#)] [[PubMed](#)]
26. Robijns, J.; Censabella, S.; Bulens, P.; Maes, A.; Mebis, J. The Use of Low-Level Light Therapy in Supportive Care for Patients with Breast Cancer: Review of the Literature. *Lasers Med. Sci.* **2017**, *32*, 229–242. [[CrossRef](#)]
27. Vasconcelos, R.M.; Sanfilippo, N.; Paster, B.J.; Kerr, A.R.; Li, Y.; Ramalho, L.; Queiroz, E.L.; Smith, B.; Sonis, S.T.; Corby, P.M. Host-Microbiome Cross-Talk in Oral Mucositis. *J. Dent. Res.* **2016**, *95*, 725–733. [[CrossRef](#)]
28. Antunes, H.S.; Wajnberg, G.; Pinho, M.B.; Jorge, N.A.N.; de Moraes, J.L.M.; Stefanoff, C.G.; Herchenhorn, D.; Araújo, C.M.M.; Viêgas, C.M.P.; Rampini, M.P.; et al. CDNA Microarray Analysis of Human Keratinocytes Cells of Patients Submitted to Chemoradiotherapy and Oral Photobiomodulation Therapy: Pilot Study. *Lasers Med. Sci.* **2018**, *33*, 11–18. [[CrossRef](#)]
29. Topaloglu, N.; Özdemir, M.; Çevik, Z.B.Y. Comparative analysis of the light parameters of red and near-infrared diode lasers to induce photobiomodulation on fibroblasts and keratinocytes: An in vitro study. *Photodermatol. Photoimmunol. Photomed.* **2021**, *37*, 253–262. [[CrossRef](#)]
30. Wagner, V.P.; Curra, M.; Webber, L.P.; Nör, C.; Matte, U.; Meurer, L.; Martins, M.D. Photobiomodulation Regulates Cytokine Release and New Blood Vessel Formation during Oral Wound Healing in Rats. *Lasers Med. Sci.* **2016**, *31*, 665–671. [[CrossRef](#)]
31. Cury, V.; Moretti, A.I.S.; Assis, L.; Bossini, P.; de Souza Crusca, J.; Neto, C.B.; Fangel, R.; de Souza, H.P.; Hamblin, M.R.; Parizotto, N.A. Low Level Laser Therapy Increases Angiogenesis in a Model of Ischemic Skin Flap in Rats Mediated by VEGF, HIF-1 α and MMP-2. *J. Photochem. Photobiol. B Biol.* **2013**, *125*, 164–170. [[CrossRef](#)] [[PubMed](#)]
32. Stepanov, Y.V.; Golovynska, I.; Golovynskiy, S.; Garmanchuk, L.V.; Gorbach, O.; Stepanova, L.I.; Khranovska, N.; Ostapchenko, L.I.; Ohulchanskyy, T.Y.; Qu, J. Red and near infrared light-stimulated angiogenesis mediated via Ca²⁺ influx, VEGF production and NO synthesis in endothelial cells in macrophage or malignant environments. *J. Photochem. Photobiol. B* **2022**, *227*, 112388. [[CrossRef](#)] [[PubMed](#)]
33. Martignago, C.C.S.; Tim, C.R.; Assis, L.; Neves, L.M.G.; Bossini, P.S.; Renno, A.C.; Avo, L.R.S.; Liebano, R.E.; Parizotto, N.A. Comparison of Two Different Laser Photobiomodulation Protocols on the Viability of Random Skin Flap in Rats. *Lasers Med. Sci.* **2019**, *34*, 1041–1047. [[CrossRef](#)] [[PubMed](#)]
34. Volpato, L.E.R.; de Oliveira, R.C.; Espinosa, M.M.; Bagnato, V.S.; Machado, M.A.A.M. Viability of Fibroblasts Cultured under Nutritional Stress Irradiated with Red Laser, Infrared Laser, and Red Light-Emitting Diode. *J. Biomed. Opt.* **2011**, *16*, 075004. [[CrossRef](#)]
35. Martignago, C.C.S.; Tim, C.R.; Assis, L.; Da Silva, V.R.; Santos, E.C.B.D.; Vieira, F.N.; Parizotto, N.A.; Liebano, R.E. Effects of red and near-infrared LED light therapy on full-thickness skin graft in rats. *Lasers Med. Sci.* **2020**, *35*, 157–164. [[CrossRef](#)]
36. Bezinelli, L.M.; Corrêa, L.; Vogel, C.; Kutner, J.M.; Ribeiro, A.F.; Hamerschlak, N.; Eduardo, C.P.; Migliorati, C.A.; Eduardo, F.P. Long-term safety of photobiomodulation therapy for oral mucositis in hematopoietic cell transplantation patients: A 15-year retrospective study. *Support Care Cancer* **2021**, *29*, 6891–6902. [[CrossRef](#)]

Disclaimer/Publisher’s Note: The statements, opinions and data contained in all publications are solely those of the individual author(s) and contributor(s) and not of MDPI and/or the editor(s). MDPI and/or the editor(s) disclaim responsibility for any injury to people or property resulting from any ideas, methods, instructions or products referred to in the content.